

Surface Wave Dispersion Measurements and Tomography From Ambient Seismic Noise in China

Xiaodong Song

**University of Illinois at Urbana-Champaign
Department of Geology
1301 W. Green St. 245 NHB
Urbana, IL 61801**

Annual Report No. 1

20 December 2007

APPROVED FOR PUBLIC RELEASE; DISTRIBUTION UNLIMITED.



**AIR FORCE RESEARCH LABORATORY
Space Vehicles Directorate
29 Randolph Rd
AIR FORCE MATERIEL COMMAND
HANSCOM AFB, MA 01731-3010**

NOTICES

Using Government drawings, specifications, or other data included in this document for any purpose other than Government procurement does not in any way obligate the U.S. Government. The fact that the Government formulated or supplied the drawings, specifications, or other data does not license the holder or any other person or corporation; or convey any rights or permission to manufacture, use, or sell any patented invention that may relate to them.

This report was cleared for public release and is available to the general public, including foreign nationals. Qualified requestors may obtain additional copies from the Defense Technical Information Center (DTIC) (<http://www.dtic.mil>). All others should apply to the National Technical Information Service.

AFRL-RV-HA-TR-2009-1019 HAS BEEN REVIEWED AND IS APPROVED FOR PUBLICATION IN ACCORDANCE WITH ASSIGNED DISTRIBUTION STATEMENT.



ROBERT J. RAISTRICK
Contract Manager



PAUL TRACY, Acting Chief
Battlespace Surveillance Innovation Center

This report is published in the interest of scientific and technical information exchange, and its publication does not constitute the Government's approval or disapproval of its ideas or findings.

REPORT DOCUMENTATION PAGE

Form Approved
OMB No. 0704-0188

Public reporting burden for this collection of information is estimated to average 1 hour per response, including the time for reviewing instructions, searching existing data sources, gathering and maintaining the data needed, and completing and reviewing this collection of information. Send comments regarding this burden estimate or any other aspect of this collection of information, including suggestions for reducing this burden to Department of Defense, Washington Headquarters Services, Directorate for Information Operations and Reports (0704-0188), 1215 Jefferson Davis Highway, Suite 1204, Arlington, VA 22202-4302. Respondents should be aware that notwithstanding any other provision of law, no person shall be subject to any penalty for failing to comply with a collection of information if it does not display a currently valid OMB control number. **PLEASE DO NOT RETURN YOUR FORM TO THE ABOVE ADDRESS.**

1. REPORT DATE (DD-MM-YYYY) 20-12-2007		2. REPORT TYPE Annual Report No. 1		3. DATES COVERED (From - To) 20-Dec-2006 to 20-Dec-2007	
4. TITLE AND SUBTITLE Surface Wave Dispersion Measurements and Tomography From Ambient Seismic Noise in China				5a. CONTRACT NUMBER FA8718-07-C-0006	
				5b. GRANT NUMBER N/A	
				5c. PROGRAM ELEMENT NUMBER 62601F	
6. AUTHOR(S) Xiaodong Song				5d. PROJECT NUMBER 1010	
				5e. TASK NUMBER SM	
				5f. WORK UNIT NUMBER A1	
7. PERFORMING ORGANIZATION NAME(S) AND ADDRESS(ES) University of Illinois at Urbana-Champaign Department of Geology 1301 W. Green St. 245 NHB Urbana, IL 61801				8. PERFORMING ORGANIZATION REPORT NUMBER	
9. SPONSORING / MONITORING AGENCY NAME(S) AND ADDRESS(ES) Air Force Research Laboratory 29 Randolph Rd. Hanscom AFB, MA 01731-3010				10. SPONSOR/MONITOR'S ACRONYM(S) AFRL/RVBYE	
				11. SPONSOR/MONITOR'S REPORT NUMBER(S) AFRL-RV-HA-TR-2009-1019	
12. DISTRIBUTION / AVAILABILITY STATEMENT Approved for Public Release; Distribution Unlimited.					
13. SUPPLEMENTARY NOTES					
14. ABSTRACT <p>We have recently performed ambient noise tomography of China using the new national China Seismic Network and surrounding global and regional stations. For most of the station pairs, we can retrieve very good Rayleigh waves from ambient noise correlations using 18-months of continuous data at all distance ranges (100 km to 5000 km) and for periods down to about 8 s. We obtain Rayleigh wave group velocity dispersion measurements using a frequency-time analysis method and construct Rayleigh wave group velocity maps for periods from 8 s to 60 s. Our preliminary dispersion maps show significant features that correlate with surface geology. Two major features stand out in particular. First, the major basins with thick sediment deposition correlate well with slow group velocities at shorter periods (10 to 20 s). The major basins, including Tarim, Junggar, Qadaim, Sichuan, Bohai, Songliao, Southern North China, and Jiangnan, are all well delineated by slow velocities. Second, variations in crustal thickness correlate with group velocities for periods around 30 s. The major trend of crust thickening from the east to west is well represented by the velocity decreases from east to west. We propose several methods to estimate the reliability and error of Rayleigh wave dispersions derived from the ambient noise.</p>					
15. SUBJECT TERMS Variational analysis, Adjoint method, Data assimilation					
16. SECURITY CLASSIFICATION OF:			17. LIMITATION OF ABSTRACT	18. NUMBER OF PAGES	19a. NAME OF RESPONSIBLE PERSON Robert Raistrick
a. REPORT UNC	b. ABSTRACT UNC	c. THIS PAGE UNC			19b. TELEPHONE NUMBER (include area code) 781-377-3726

Table of Contents

1. Summary	1
2. Introduction	2
3. Data and Method	3
4. Results and Discussion	5
4.1. Ambient Noise Correlations and Dispersion Measurements	5
4.2. Surface-Wave Tomography	8
4.3. Robustness of Measurements	12
5. Conclusions	12
References	15

1. SUMMARY

Recent laboratory and theoretical studies have shown that the Green functions of a structure can be obtained from the cross-correlation of diffuse wavefields. The idea has now found rapid applications in seismology, in particular, surface waves have been found to be most easily retrievable from the cross-correlations of seismic coda or ambient noise. Dispersion measurements made on the estimated Green functions present significant advantages over traditional measurements that are based on earthquakes with limited distribution. The method is particularly useful in surface-wave path calibration and tomographic mapping in aseismic regions and at short periods (below 20 s). We have recently performed ambient noise tomography of China using the new national China Seismic Network and surrounding global and regional stations. For most of the station pairs, we can retrieve very good Rayleigh waves from ambient noise correlations using 18-months of continuous data at all distance ranges (100 km to 5000 km) and for periods down to about 8 s. The combination of stations achieves good and relatively uniform coverage for most parts of China. We obtain Rayleigh wave group velocity dispersion measurements using a frequency-time analysis method and construct Rayleigh wave group velocity maps for periods from 8 s to 60 s. Our preliminary dispersion maps show significant features that correlate with surface geology. Two major features stand out in particular. First, the major basins with thick sediment deposition correlate well with slow group velocities at shorter periods (10 to 20 s). The major basins, including Tarim, Junggar, Qadain, Sichuan, Bohai, Songliao, Southern North China, and Jiangnan, are all well delineated by slow velocities. Second, variations in crustal thickness correlate with group velocities for periods around 30 s. The major trend of crust thickening from the east to west is well represented by the velocity decreases from east to west. We propose several methods to estimate the reliability and error of Rayleigh wave dispersions derived from the ambient noise.

2. INTRODUCTION

The overall objective of this project is to obtain surface wave dispersion measurements from ambient seismic noise correlations of the Chinese backbone stations (CNSN) and global and temporary stations in the surrounding regions, and use these measurements to produce surface wave dispersion maps of China. The ultimate goal is to improve capability for detecting and monitoring small events using the Ms: mb discriminant by improving path calibration of surface wave propagation, particularly in aseismic areas. Below I give a brief introduction to ambient noise tomography. I then describe the data used in this study and the procedures of data processing in Section 3. Results are presented in Section 4 and concluding remarks are in Section 5. This project is in collaboration with Dr. Sihua Zheng (China Earthquake Administration) and Dr. Mike Ritzwoller (University of Colorado at Boulder). The latest results have been presented in the AGU 2007 Fall Meeting as an invited paper (Song et al., 2007).

Recent theoretical and laboratory studies have shown that the Green functions of a structure can be obtained from the cross-correlation of diffuse wavefields (Weaver and Lobkis, 2001; Lobkis and Weaver, 2001; Derode et al., 2003; Snieder 2004; Wapenaar, 2004; Larose et al., 2004; see also reviews by Larose et al, 2006 and Campillo, 2006). The basic idea is that linear waves preserve, regardless of scattering, a residual coherence that can be stacked and amplified to extract coherent information between receivers (Weaver, 2005). The basic approach can be traced back much earlier studies of random fields in seismology (Aki, 1957; Toksoz, 1964; Claerbout, 1968), in helioseismology (Rickett and Claerbout, 1995), and in acoustics (Eagle, 1981; Weaver, 1982). The idea has now found rapid applications in seismology. In particular, surface waves have been found to be most easily retrievable from the cross-correlations of seismic coda (Campillo and Paul, 2003; Paul et al., 2005) or ambient noise (Shapiro and Campillo, 2004; Shapiro et al., 2005; Sabra et al., 2005a, 2005b) between two stations, although a retrieval of the P waves has been reported (Roux et al., 2005).

Tomographic studies of surface waves from ambient noise correlations were first conducted by Shapiro et al. (2005) and Sabra et al. (2005b) in S. California. The results were quite impressive, showing nice correlations between surface wave speeds and major geological units. The approach has now been rapidly applied in different regions of the world: Southwest China (Yao et al., 2006), Europe (Yang et al., 2007), and S. Korea (Kang and Shin, 2006; Cho et al., 2006; Yoo et al., 2006).

The ambient noise tomography overcomes some of the important limitations of conventional methods based on energetic sources (mainly earthquakes). (1) The data coverage is limited by source distribution. Earthquake distribution is very un-uniform, resulting in very un-uniform sampling. This is particularly a problem in aseismic regions. (2) Tomography requires knowledge of earthquake location and perhaps focal mechanisms. The knowledge is not accurate. (3) Constrained by source distributions, higher frequency signals are attenuated by intrinsic attenuation and the scattering of the media when the path is long, limiting the resolution of seismic imaging.

3. DATA AND METHOD

The data we used include the recent Chinese backbone stations and global stations in the surrounding regions (Fig. 1). The Chinese backbone network consists of 48 stations, which are distributed fairly uniformly in China. We used 47 of the 48 stations, because one station (Xisha) has no data. The network has been referred to as China National Seismic Network (CNSN), China National Digital Seismic Network (CNDSN), Center of China Digital Seismic Network (CCDSN) stations, and China Seismic Network (CSN). We refer here as China National Seismic Network (CNSN). Except for stations of the China Digital Seismic Network (CDSN), which was established between China/State Seismological Bureau and the US Geological Survey in 1986, most of the new stations started operating in early 2000. The bandwidths of the instruments are from 20 Hz to over 120 s. Recently, 25 CNSN stations (including 10 CDSN stations) have been designated as international exchange stations. Data access to the rest (23) of the CNSN stations is more limited.

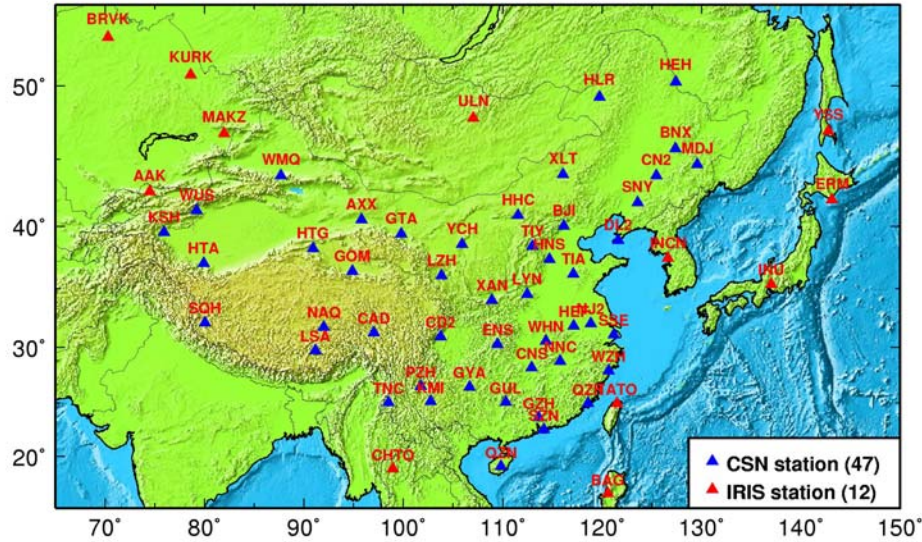


Fig. 1. Distribution of China Seismic Network stations and global stations used in this study.

We use techniques and software that are developed by Ritzwoller and co-workers. The basic techniques have been discussed in great detail by Bensen et al. (2007). Below is an outline of the data processing and imaging steps we use. The first step is data pre-processing, cross-correlation, and stacking. The pre-processing includes clock synchronization (some Chinese stations use local time instead of GMT), removal of instrument response, time-domain filtering, temporal normalization and spectral whitening. The purpose is to reduce the influence of earthquake signals and instrument irregularities and to enhance the strength and bandwidth of ambient noise in the cross-correlations. The result of the first step is the empirical Green function from the cross-correlation. Second, if the signal-to-noise ratio (SNR) is large enough, group speed curves are measured in each period band based on a frequency-time analysis (FTAN) (Ritzwoller and Levshin, 1998). Third, repeat dispersion measurement from ambient

seismic noise for different time periods and use the result to estimate measurement uncertainties. Similarly, if there are dense arrays of stations as in North China, S. Korea, and Japan, we can repeat dispersion measurements between a remote station and stations that are close by to estimate measurement uncertainties. Fourth, the final stage of ambient noise tomography is group speed tomography itself. Dispersion measurements between station-pairs can be used to produce group speed maps exactly as earthquake data are used.

4. RESULTS AND DISCUSSION

4.1. Ambient Noise Correlations and Dispersion Measurements

Our analysis is based on a total of 18 months of continuous data that we have collected. The data cover the periods from Nov. 2003 through Oct. 2004 and from Jan. 2007 through June 2007. For most of the station pairs, we can retrieve very good Rayleigh waves from ambient noise correlations. Fig. 2 shows typical examples of empirical Green functions of Rayleigh waves retrieved from ambient noise correlations. The cross-correlations show strong arrivals at different settings (near the coast or well into the continental interior) and at both relatively low frequencies (20-50 s) and high frequencies (5-20 s).

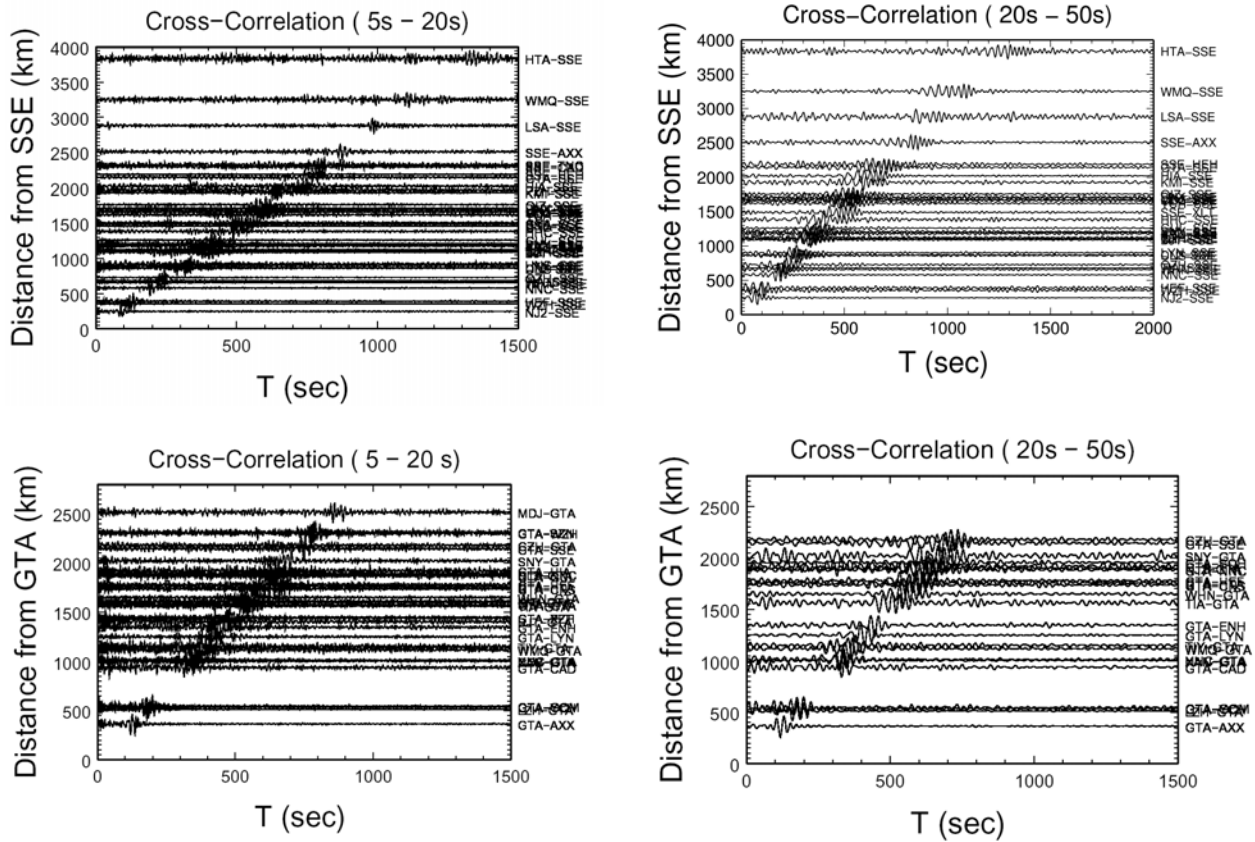


Fig. 2. Ambient noise cross-correlations relative to two CNSN stations: one near the coast (SSE, Shanghai) (upper panels) and one in the continental interior (GTA, Gangsu Province) (lower panels). The plot shows cross-correlations of the station with all the other CNSN stations using 1 year of data. The cross-correlations are filtered at two frequency bands (5 to 20 s and 20 to 50 s).

For pairs with Rayleigh wave SNR >10 , we measured group velocity dispersion curves using the FTAN method (Ritzwoller and Levshin, 1998). The measurement is very stable. Fig. 3 shows two examples of Rayleigh wave group velocity dispersion measurements from the empirical Green function retrieved. Note the group velocity measurements can extend to periods of 10 s or shorter even for station pairs that are separated over thousands of kilometers. The AXX-QIZ path shows group velocities very similar to the predictions from a global 3D model based on earthquake data (Shapiro and Ritzwoller, 2002). However, the HTA-BRVK path, which samples the Tarim Basin, shows

significantly lower group velocities at short periods (below 30 s). This is consistent with thickness sediments of the basin (see discussion below).

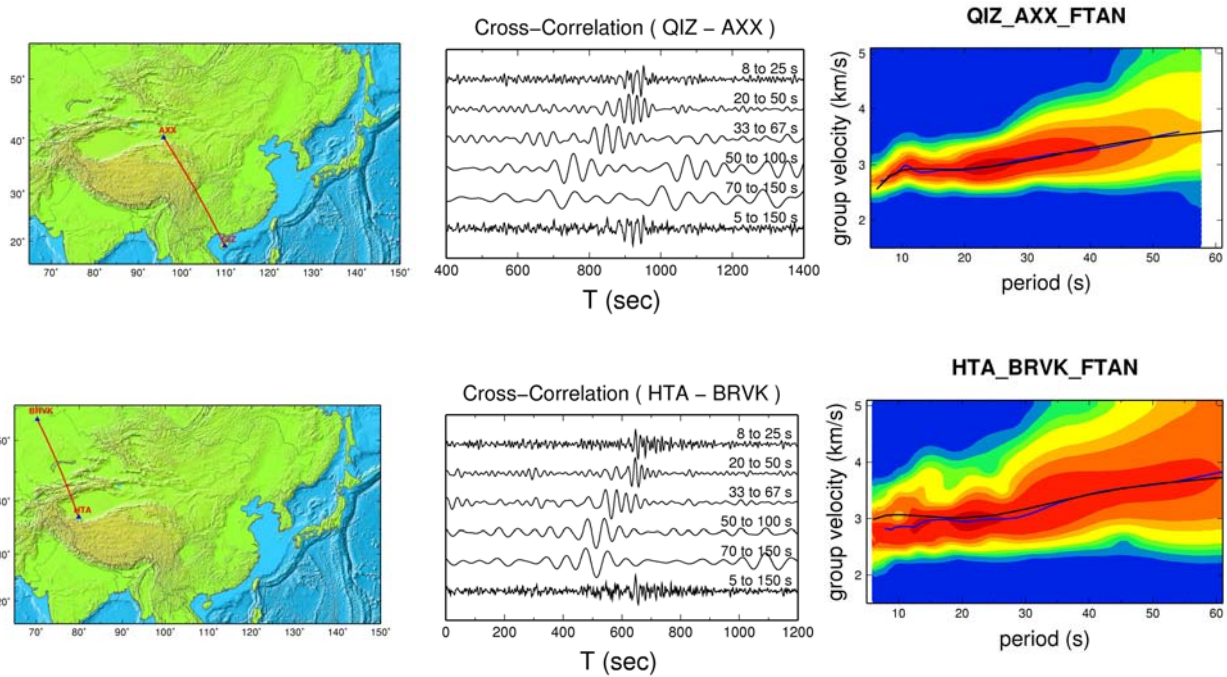


Fig. 3. Examples of station-station cross-correlations and frequency-time analysis (FTAN) (Ritzwoller and Levshin, 1998) to retrieve dispersion curves (blue lines) for Rayleigh waves of station pair AXX-QIZ (upper panels) and HTA-BRVK (lower panels). From left to right are map of the ray path, the Green function filtered at different periods, and FTAN plot, respectively. In the FTAN plot, the black curve is the prediction from the 3-D model by Shapiro and Ritzwoller (2002), which is used for phase-matching filter in the data analysis and for comparison with actual measurement (in blue).

We have obtained thousands of dispersion measurements with $\text{SNR} > 10$ for periods 8 s to 70 s (Fig. 4). The SNR is the signal-to-noise ratio defined as the peak amplitude of the Rayleigh wave divided by the rms amplitude of the background noise. The best observed frequency band is 10 to 30 s with retrievals of 50 to 80% of the possible pairs.

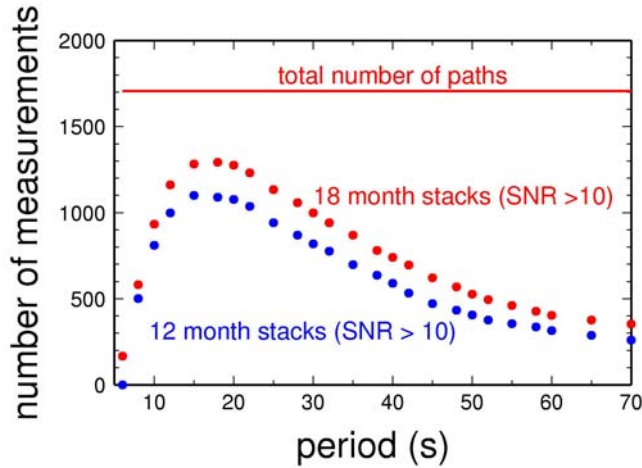


Fig. 4. Number of dispersion measurements obtained for different periods in this study. The total number of possible paths (station pairs) is about 1700. The numbers of measurements obtained from 18-months of continuous data are in red dots. The numbers show about 20% of improvement over the numbers of measurements obtained using only 12-months of data (blue dots). Rayleigh waves are retrieved over a wide frequency band (8 to 70 s). The best observed frequencies are 10 to 30 s.

4.2. Surface-Wave Tomography

Using the dispersion measurements we have made, we obtained tomographic maps of group velocities at frequencies from 8 s to 60 s (Fig. 5). The results show some remarkable features that correlate with large-scale geological structures of China. Major basins are well delineated with low velocities at periods 8 s and 20 s, including Bohai Basin (North China Basin), Sichuan Basin, Qaidam Basin, and Tarim Basin. The Yangtze Craton also shows up well with high velocities. At a longer period (25-50 s), the group velocity maps display striking bi-modal distribution with high velocity in the east and low velocity in the west, which corresponds very well the thinner crust in the east and much thicker crust in the west (e.g. Liang et al., 2004). The NNE-SSW trending boundary between fast and slow velocities (around longitude 108°E) coincides with the sharp topography change and with the well-known Gravity Lineation.

Fig. 6 shows side-by-side comparison between the group velocity map at 15 s and sediment thickness. Fig. 7 shows comparison between the group velocity map at 30 s and the crustal thickness. The correlations are quite remarkable if we compare the group velocities along a certain profile of interest (Fig. 8).

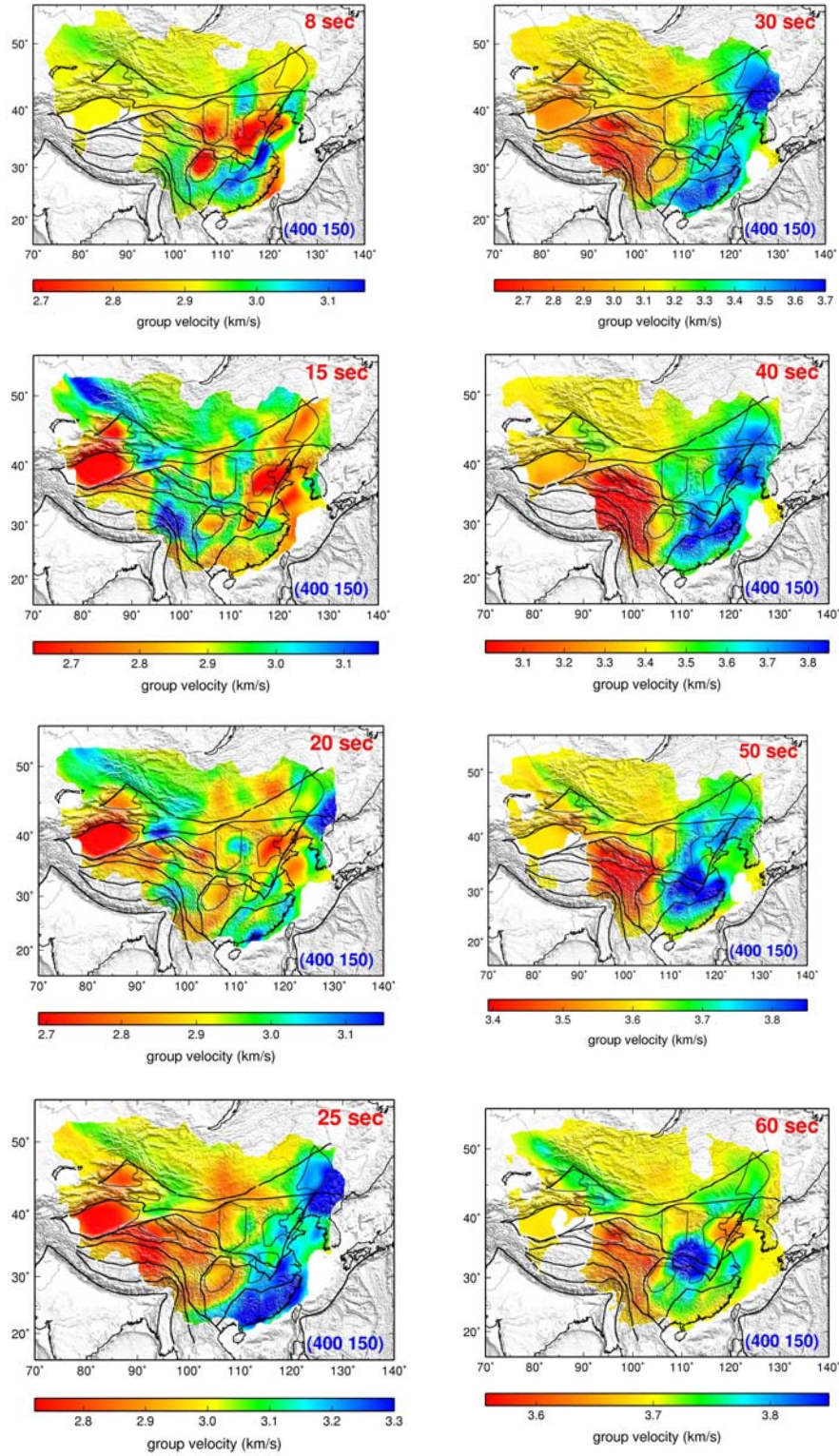


Fig. 5. Rayleigh wave group velocities obtained in this study. Show are the maps at periods 8, 15, 20, 25, 30, 40, 50, 60 s, respectively.

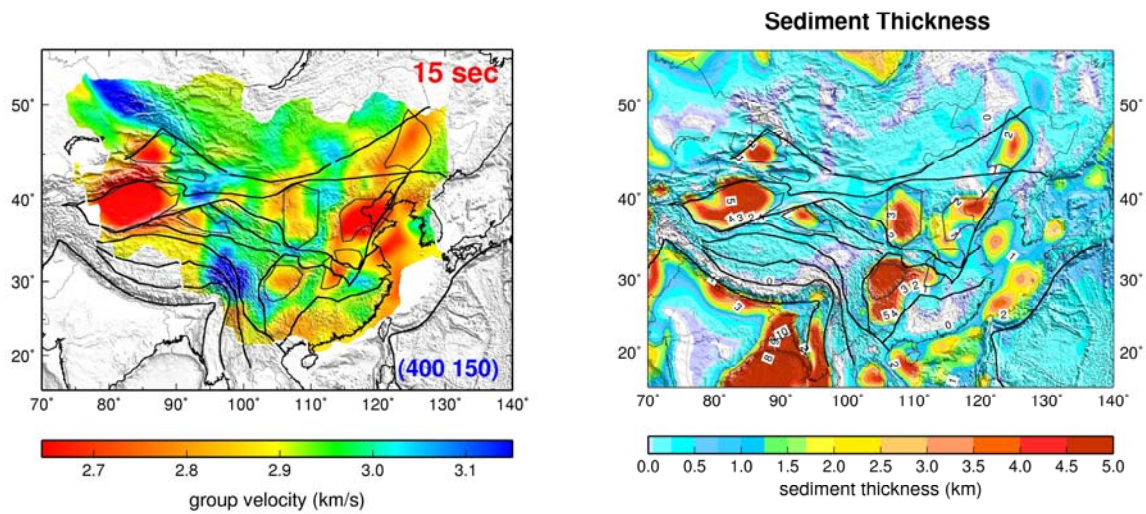


Fig. 6. Comparison of group velocity map at 15 s (left) and sediment thickness (right). Plotted in the background are major block boundaries and basin outlines (Liang, Song and Huang, JGR, 2004). The major basins (including Tarim, Junggar, Qadaim, Sichuan, Bohai, Songliang, Southern North China, Jiangang) are well delineated by slow velocities.

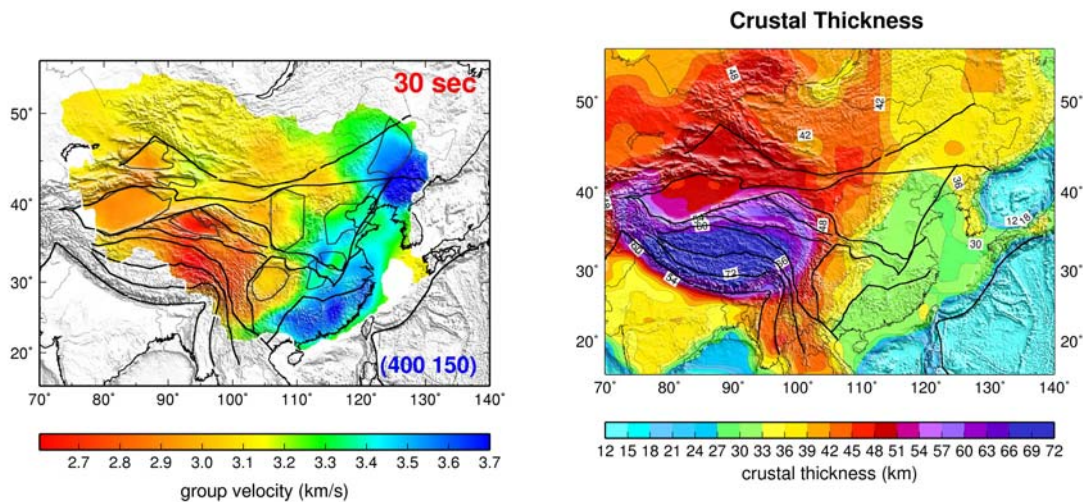
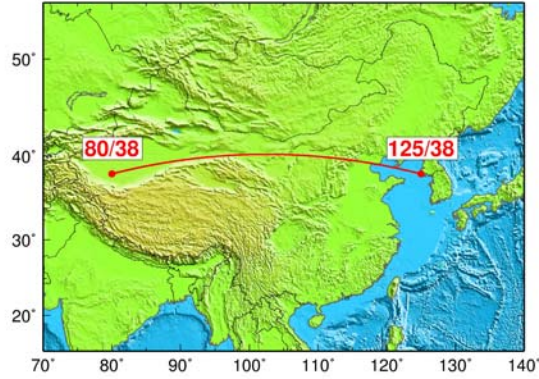
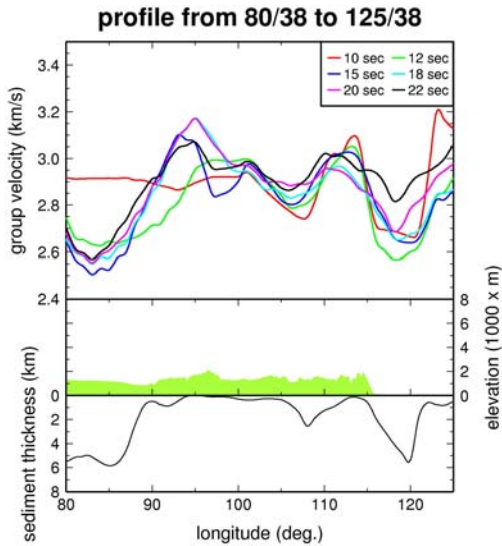


Fig. 7. Comparison of group velocity map at 30 s (left) and crustal thickness (right). The major trend of crust thickening from the east to west (right) is well represented by the velocity decreases from east to west (left).

A)



B)



C)

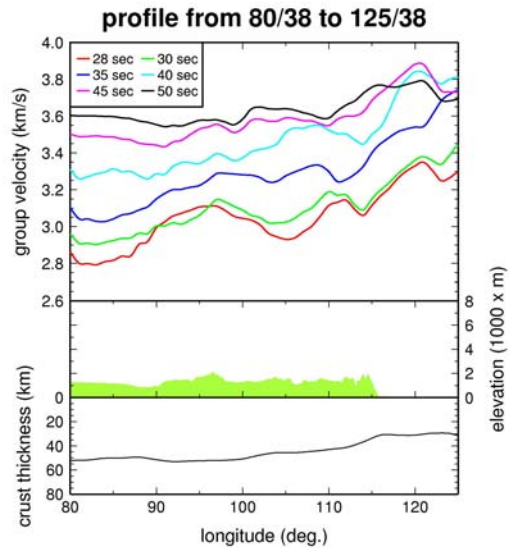


Fig. 8. Comparison of group velocities and sediment thickness and crustal thickness along the selected path. (A) The selected profile along latitude 38 deg passes three major basins (Tarim, Ordos, and Bohai). (B) The three major basins correlate well with slow velocities at periods 10 to 20 s. The surface elevation (middle, shaded green) is plotted for reference. The elevation and sediment thickness are plotted using the same scale. (C) The general trend of decreasing crustal thickness from west to east is well represented by increasing group velocities at 30 s. However, the group velocity shows more structure than the smooth crustal thickness curve from the global reference model (CRUST 2.0), suggesting likely more complex Moho structure. At period 50 s, the trend is not observable any more as the surface waves sample deeper into the mantle.

4.3. Robustness of Measurements

For a diffuse field, it has been proved that cross-correlation yields the Green function between the stations, as discussed in the introduction. If the field is not diffuse, how can we validate that the Rayleigh waves we have obtained from the cross-correlation are the true solution of the media. If it is not a true solution, what is the error of the estimate? Some ideas have been proposed before. (1) Comparing the cross-correlation with surface wave generated by an earthquake along the same path. (2) Comparing correlations using data from different seasons of the year. Because there will be different noise sources from the oceans, the consistency of the correlations gives a measure of stability and error of the Green function.

We propose further validation methods. (3) Model-based validation. The surface wave tomographic maps can be used to test how good the models are. In this regard, the discussion above on comparing the tomographic maps with geological structure and processes is particularly relevant. A good model should be consistent with well-know geological features. (4) Temporal comparison: Comparing correlations with different sliding time windows (Fig. 9). For noise sources that may not be seasonal, the method provides a way to measure the variations of different time windows. The dispersion curves are very stable. Longer time windows improve the stability at longer periods, but also at the shorter periods. (5) Spatial comparison: Comparing correlations for pairs along similar paths (Fig. 10). Green functions between a station to two close stations should be similar as they sample similar structure. This is indeed the case for YCH to GZH and YCH to SZN. YCH falls on the great circle path passing GZH and SZN, which are relatively close to each other.

5. CONCLUSIONS

We have obtained Rayleigh wave group velocity measurements using ambient noise correlations of 18 months of continuous data of CNSN and some global stations. The Rayleigh waves can be retrieved from about 8 s to 70 s. The best observed frequency band is 10 to 30 s with retrieval rate of 50 to 80% of the pairs. Rayleigh group velocity

tomographic maps show remarkable correlations with major tectonic features of china. The correlations between the tomographic models and the tectonic features provide an important validation of the methodology, the dispersion measurements, and the tomographic results. Studies of the temporal and spatial consistency also suggest that our measurements are robust. Further studies will quantify the errors of the measurements and tomographic models.

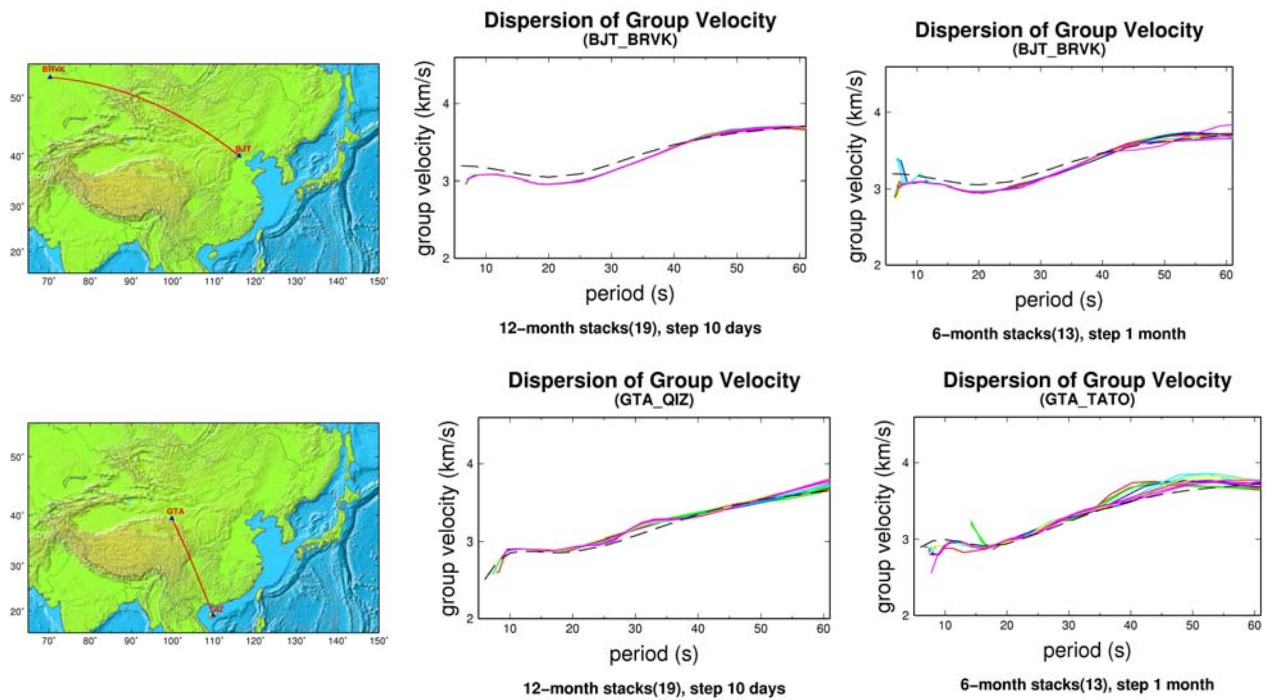


Fig. 9. Comparison of dispersion curves from different time windows. Two examples are BJT and BRVK pair (upper panels) and GTA and QIZ pair (lower panels). For each path from left to right are the map of the path, dispersion curves obtained from 12-months of data with a sliding time window of 10 days (total of 19 curves), and dispersion curves obtained from 6-months of data with a sliding time window of 1 month (total of 13 curves).

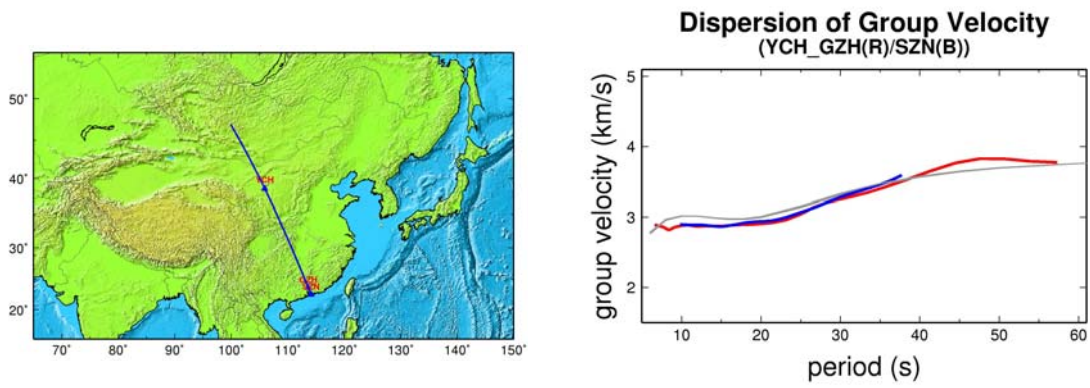


Fig. 10. Comparison of dispersion curves between YCH and GZH (red) and between YCH and SZN (blue). The two paths are very similar. The group velocities are also very similar for periods where they overlap (10 to 40 s).

REFERENCES

- Aki, K. (1957), Space and time spectra of stationary stochastic waves with special reference to microtremors, *Bull. Earthq. Res. Inst.* 35, 415-456.
- Benson, G., M. Ritzwoller, M. Barmin et al., Processing seismic ambient noise data to obtain reliable broad-band surface wave dispersion measurements, *Geophys. J. Int.*, in press, 2007.
- Campillo, M. Phase and correlation in Random Seismic Fields and the reconstruction of the Green function, *Pure Appl. Geophys.*, 163, 475-502, 2006.
- Campillo M. and A. Paul, Long-range correlations in the diffuse seismic coda, *Science*, 299, 547-549, 2003.
- Cho, K. H., R. B. Herrmann, C. J. Ammon and K. Lee (2007). Imaging the upper crust of the Korean peninsula by surface-wave tomography, *Bull. Seism. Soc. Am.* (in press).
- Claerbout, J.F., Synthesis of a layered medium from its acoustic transmission response, *Geophys.*, 33(2), 264-269, 1968.
- Derode, A., Larose, E., Tanter M, et al., Recovering the Green's function from field-field correlations in an open scattering medium (L), *J. Acoust. Soc. Amer.* 113 (6), 2973-2976, 2003.
- Eagle, D., Diffuse wave fields in solid media, *J. Acoustic. Soc. Am.* 70(2), 476-480, 1981.
- Kang, T.S. and J.S. Shin, Surface-wave tomography from ambient noise of accelerograph networks in southern Korea, *Geophys. Res. Lett.*, 33 (17): Art. No. L 17303, 2006.
- Liang, C.T., X.D. Song, J.L. Huang, Tomographic inversion of Pn travel times in China, *J. Geophys. Res.*, 109, B11304, doi: 10.1029/2003JB002789, 2004.
- Larose E, Derode A, Campillo M, et al., Imaging from one-bit correlations of wideband diffuse wave fields, *J. APPL. PHYS.* 95 (12) 8393-8399, 2004.
- Larose E, Margerin L, Derode A, et al., Correlation of random wavefields: An interdisciplinary review, *Geophys.* 71 (4): S111-SI21 Suppl. S JUL-AUG 2006.
- Lobkis, O.I., and R.L. Weaver, On the emergence of the Greens function in the correlations of a diffuse field, *J. Acoust. Soc. Am.*, 110, 3011-3017, 2001.
- Paul, A., M Campillo, L. Margerin and E. Larose (2005) Empirical synthesis of time-asymmetrical Greens functions from the correlation of coda waves, *J. Geophys. Res.*, 110, B08201, doi: 10.1029/2004JB0035231.
- Rickett, J. and J.F. Claerbout, Acoustic daylight imaging via spectral factorization: Helioseismology and reservoir monitoring, *the Leading Edge*, 18, 957-960, 1999.
- Ritzwoller, M.H. and A.L. Levshin, Eurasian surface wave tomography: Group velocities, *J. Geophys. Res.*, 103, 4839-4878, 1998.
- Roux, P., K.G. Sabra, P. Gerstoft, W.A. Kuperman, and M.C. Fehler, P-waves from cross correlation of seismic noise, *Geophys. Res. Lett.*, L19303, 2005.
- Sabra, K.G., P. Gerstoft, P. Roux, W.A. Kuperman, and M.C. Fehler, Extracting timedomain Green's function estimates from ambient seismic noise, *Geophys. Res. Lett.* 32, doi: 10.1029/2004GL021862, 2005a.
- Sabra, K.G., P. Gerstoft, P. Roux, W.A. Kuperman, and M.C. Fehler, Surface wave tomography from microseisms in Southern California, *Geophys. Res. Lett.*, 2005b.
- Shapiro, N.M. and M.H. Ritzwoller, Monte-Carlo inversion for a global shear velocity model of the crust and upper mantle, *Geophys. J. Int.*, 151, 88-105, 2002.

- Shapiro, N.M. and M. Campillo, Emergence of broadband Rayleigh waves from correlations of the ambient seismic noise, *Geophys. Res. Lett.*, 31, L07614, doi: 10.1029/2004GL019491, 2004.
- Shapiro, N.M. M. Campillo, L. Stehly, and M.H. Ritzwoller, High resolution surface wave tomography from ambient seismic noise, *Science*, 307(5715), 1615-1618, 2005.
- Song, X.D., S.H. Zheng, X.L. Sun, M.H. Ritzwoller, Y.J. Yang, Surface wave dispersion measurements and tomography from ambient seismic noise in China, Fall AGU Meet., 2007.
- Snieder, R., Extracting the Green's function from the correlation of coda waves: A derivation based on stationary phase, *Phys. rev. E*, 69, 046610, 2004.
- Wapenaar K., Retrieving the elastodynamic Green's function of an arbitrary inhomogeneous medium by cross correlation, *Phys. Rev. Lett.*, 93 (25), 254301, doi:10.1103/PhysRevLett.93.254301, 2004.
- Weaver, R.L., Information from Seismic Noise, *Science*, 307, 1568-1569, 2005.
- Weaver, R.L., Lobkis, O.I. Ultrasonics without a source: Thermal fluctuation correlations at MHz frequencies, *Phys. Rev. Lett.*, 87(13), 134301, doi:10.1103/PhysRevLett.87.134301, 2001.
- Yang, Y.J., M.H. Ritzwoller, A.L. Levshin, and N.M. Shapiro, Ambient noise Rayleigh wave tomography across Europe, *Geophys. J. Int.* (2007)168, 259-274 doi: 10.1111/j.1365-246X.2006.03203.x
- Yao, H.J., R.D. van der Hilst, and M.V. de Hoop (2006) Surface-wave array tomography in SE Tibet from ambient noise and two-station analysis - I. phase velocity maps, *Geophys. J. Int.*, 166(2) 732-744.
- Yoo, H. J., R. B. Herrmann, K. H. Cho and K. Lee, Imaging the three-dimensional crust of the Korean peninsula by joint inversion of surface-wave dispersion and teleseismic receiver functions, *Bull. Seism. Soc. Am.*, in press, 2007.